



2003

Air-sea interaction processes observed from buoy and propagation measurements during the red experiment

Frederickson, Paul A.



Calhoun is a project of the Dudley Knox Library at NPS, furthering the precepts and goals of open government and government transparency. All information contained herein has been approved for release by the NPS Public Affairs Officer.

**Dudley Knox Library / Naval Postgraduate School
411 Dyer Road / 1 University Circle
Monterey, California USA 93943**

9.3 AIR-SEA INTERACTION PROCESSES OBSERVED FROM BUOY AND PROPAGATION MEASUREMENTS DURING THE RED EXPERIMENT

Paul A. Frederickson¹, Kenneth L. Davidson¹, Kenneth D. Anderson², Stephen M. Doss-Hammel² and Dimitris Tsintikidis²

¹Naval Postgraduate School, Monterey, CA

²SPAWAR Systems Center, San Diego, CA

1. INTRODUCTION

In recent years researchers have spent much effort towards gaining an understanding of the complex physical mechanisms through which the atmosphere and ocean interact with each other. This is due to the fact that knowledge of air-sea exchanges is important for a wide range of applications, such as the diverse topics of global climate modeling and near-horizon electromagnetic (EM) wave propagation assessment and prediction. EM propagation through the atmosphere is highly dependent upon the vertical profiles of air temperature and humidity and the horizontal variations in these profiles. It is well known that under most conditions these near-surface scalar profiles depend upon the turbulent air-sea fluxes. Traditional Monin-Obukhov similarity (MOS) theory has been used to successfully predict near-surface profiles over the ocean for most, but not all, stability conditions. It is also becoming increasingly clear that ocean waves influence near-surface profiles, although an understanding of the exact mechanisms through which this occurs and parameterizations to describe these processes so far have remained elusive (e.g. Hare et al. 1997; Hirstov et al. 1998).

The Roughness and Evaporation Duct (RED) experiment was conducted in the fall of 2001 with the goal of examining the applicability of existing approaches to modeling air-sea interaction mechanisms and their resulting effects on EM propagation, and ultimately to develop new and improved parameterizations. The RED Experiment was intended to focus especially on high wind and high wave conditions in a region with large temperature and humidity gradients. For this reason the experiment was held along the windward coast of Oahu, Hawaii, in August and September 2001. Mean and turbulent meteorological and ocean wave properties were measured from several platforms at different locations during the experiment, while concurrent microwave and electro-optical (EO) propagation measurements were obtained along propagation paths originating at sea from the Research Platform *FLIP* and terminating at the shore. Readers desiring further information on the RED Experiment are referred to the paper by Anderson et al. (2003) included in these proceedings.

In this paper we will examine the use of existing bulk models in predicting near-surface profiles over the ocean and explore the possible effects of surface waves upon these profiles and their ultimate impact on near-horizon microwave propagation. Directly measured vertical profiles of air temperature and humidity obtained on a buoy are examined with respect to concurrent surface wave and microwave propagation data. The results of this analysis indicate that existing bulk models based on traditional MOS theory work reasonable well in describing the near-surface profiles and microwave propagation over a swell-dominated sea in unstable conditions, but that there are possible significant surface wave effects that are not included in current models.

2. DATA COLLECTION AND PROCESSING

2.1 The NPS Buoy

During the RED Experiment the Naval Postgraduate School (NPS) deployed its research 'Flux' Buoy at the mid-point of the optical propagation path (see Figure 1) and data were successfully collected between 22 August and 18 September 2001. The buoy's onboard sensors measured mean wind speed and direction at 4.15 meters above the surface and air temperature and relative humidity at 0.71, 1.04, 2.06 and 4.08 meters (see Figure 2). Atmospheric pressure data were measured at 0.4 m and the sea surface temperature

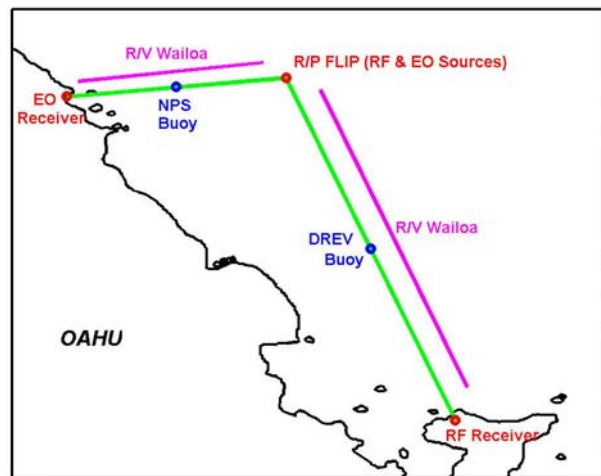


Figure 1. Map of the RED Experiment area off the windward coast of Oahu, Hawaii, showing the locations of the R/P *FLIP*, the NPS Flux Buoy and the radio-frequency (RF) and electro-optical (EO) receiver sites.

*Corresponding author address: Paul A. Frederickson, Department of Meteorology, Naval Postgraduate School, 589 Dyer Road, Room 254, Monterey, CA 93943-5114; e-mail: pafreder@nps.navy.mil

measurements were obtained from a floating thermistor mounted alongside the buoy hull. These data were averaged over successive 1 minute intervals and then stored in the on-board buoy data acquisition computer and sent by telemetry to a shore station. During post-processing these mean data were averaged over 5 minute intervals corresponding to the SSC microwave propagation data collection times and were then used as inputs to the NPS bulk model and a propagation model, as described in the next section. High frequency measurements of the 3-dimensional wind speed and air temperature were also obtained from a sonic anemometer and fluxes were computed from these data using both the eddy-correlation and inertial-dissipation methods. These flux data are not included in this paper but will be discussed in the oral presentation.

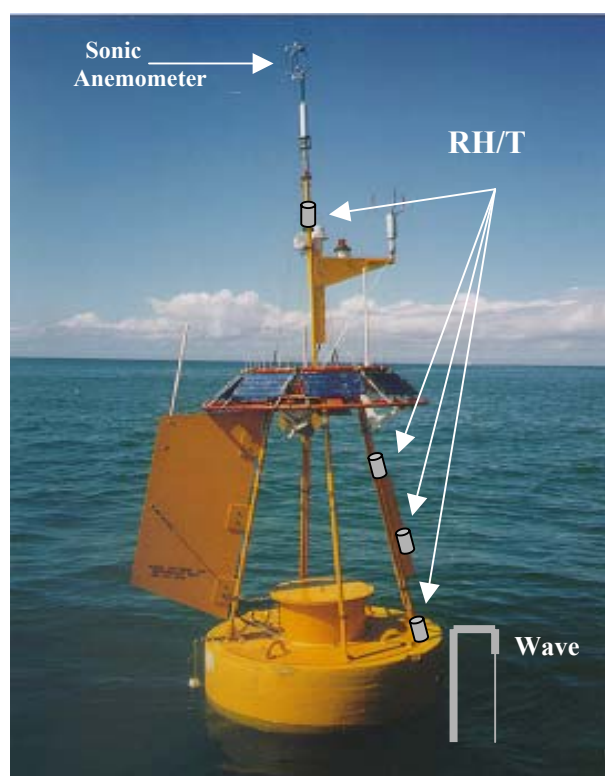


Figure 2. Photograph of the NPS Flux Buoy showing the locations of the sonic anemometer, relative humidity and temperature profile sensors, and the wave-wire staff.

Three-dimensional linear and angular buoy motion data were obtained from a Crossbow Dynamic Measurement System (DMU) located within the buoy hull. These data were sampled at 10 Hz and during post-processing were used to motion-correct the sonic anemometer data and to compute spectral wave data and wave statistics, such as significant wave height (H_s), peak period and peak swell direction. The buoy responds to waves with periods greater than about 1.67 s, and therefore the computed wave parameters represent the swell conditions and do not resolve the wind-generated capillary waves. Wave wires having the capability of

resolving these short period waves were operational on the buoy, but these data have not yet been thoroughly analyzed and are not included in this paper.

2.2 Microwave Propagation Measurements and Modeling

SPAWAR Systems Center, San Diego (SSC-SD) obtained microwave propagation loss measurements over a propagation path that roughly paralleled the windward coast of Oahu (see Figure 1). S-, X- and Ku-band (3.0, 9.7 and 17.7 GHz, respectively) transmitters were mounted at two different height levels on the R/P *FLIP*, nominally at 5 and 13 m above the surface. The receiver antenna was at a shore location on the Mokapu Peninsula at a nominal height of 4.6 m above mean sea level. The propagation path was 25.77 km in length and, except for a few meters near the receiver, was entirely over water. The propagation measurements were made over 5 minute intervals and alternated between the three frequencies and two height levels, therefore each was measured once every half hour. Further details on the propagation measurements can be found in the paper by Anderson et al. (2003).

Propagation loss values were modeled using the Advanced Propagation Model (APM) Version 1.3, developed by SSC-SD (Barrios 2002). APM is a hybrid propagation model, incorporating parabolic equation (PE) and ray-optic modeling techniques to achieve high accuracy with great computational speed. However, for the ranges and heights used in this study APM exclusively used PE methods. Bulk vertical modified refractivity profiles computed by the NPS evaporation duct model from flux buoy data were used as environmental inputs to run APM. The receiver height was adjusted for tidal variations and the transmitter heights were adjusted for waterline variations in *FLIP*. The APM calculations were performed assuming no winds and gaseous absorption was computed from the buoy meteorological data.

3. THE BULK EVAPORATION DUCT MODEL

In this study we used the NPS bulk evaporation duct model to produce estimates of near-surface scalar profiles (temperature, T , specific humidity, q , and modified refractivity, m) from the mean buoy measurements. Since it includes as one component a modified form of the surface renewal theory of Liu, Katsaros and Businger (1979), the NPS model is often referred to in the propagation community as belonging to the 'LKB' class of bulk models. As discussed above, modified refractivity profiles from the NPS model are used as inputs to APM to produce propagation loss estimates that could be compared to the actual microwave measurements.

The NPS evaporation duct model uses a modified version of the TOGA-COARE bulk model (Fairall, et. al, 1996) to estimate the surface layer scaling parameters for temperature (T_s) and specific humidity (q_s) and the

Obukhov length scale (L) from mean input values of wind speed, air and sea temperature, relative humidity and pressure. The near-surface profiles of temperature and specific humidity (from 0 to 50 m) are then computed from these scaling parameters using empirically determined scalar profile functions of stability (z/L). Vertical profiles of modified refractivity can then be computed from the estimated T and q profiles and a pressure profile obtained by assuming a hydrostatic atmosphere. The evaporation duct height is determined by finding the height where the lowest local minima in the m profile occurs. Readers desiring a more detailed description of the NPS bulk model are referred to Frederickson et al. (2000).

4. RESULTS

4.1 Profile Results

In this section we examine the effects of ocean waves on the near-surface profiles of air temperature and specific humidity. The stability functions used in bulk models, including the NPS model, were originally determined over land and therefore obviously neglect the effects that surface waves would have on over-water scalar profiles. As stated previously, it is known that

wave-induced vertical mixing does influence the near-surface profiles within a thin wavy boundary layer (e.g. Hare et al. 1997; Hirstov et al. 1998). Since wave effects are not currently included in bulk models, deviations between measured scalar profile values near the surface and bulk profile estimates may indicate the results of wave influences on the profiles.

The direct measurement of atmospheric profiles is very difficult, especially over the ocean, due to the need to resolve very small differences in the measured quantities between the height levels. All the buoy temperature/humidity sensors were carefully calibrated both before and after the experiment and they appeared to maintain their calibrations quite well over the course of the deployment. Nevertheless, we cannot claim accuracies of greater than about 0.1 °C in air temperature and 0.05 g/kg in specific humidity. With this accuracy we can, however, examine the trends in the measured-bulk differences at the different height levels as a function of significant wave height and wind speed to gain insight into the effect of swell and wind waves on near surface scalar profiles.

In Figure 3 differences between measured values of air temperature and specific humidity from the NPS buoy at

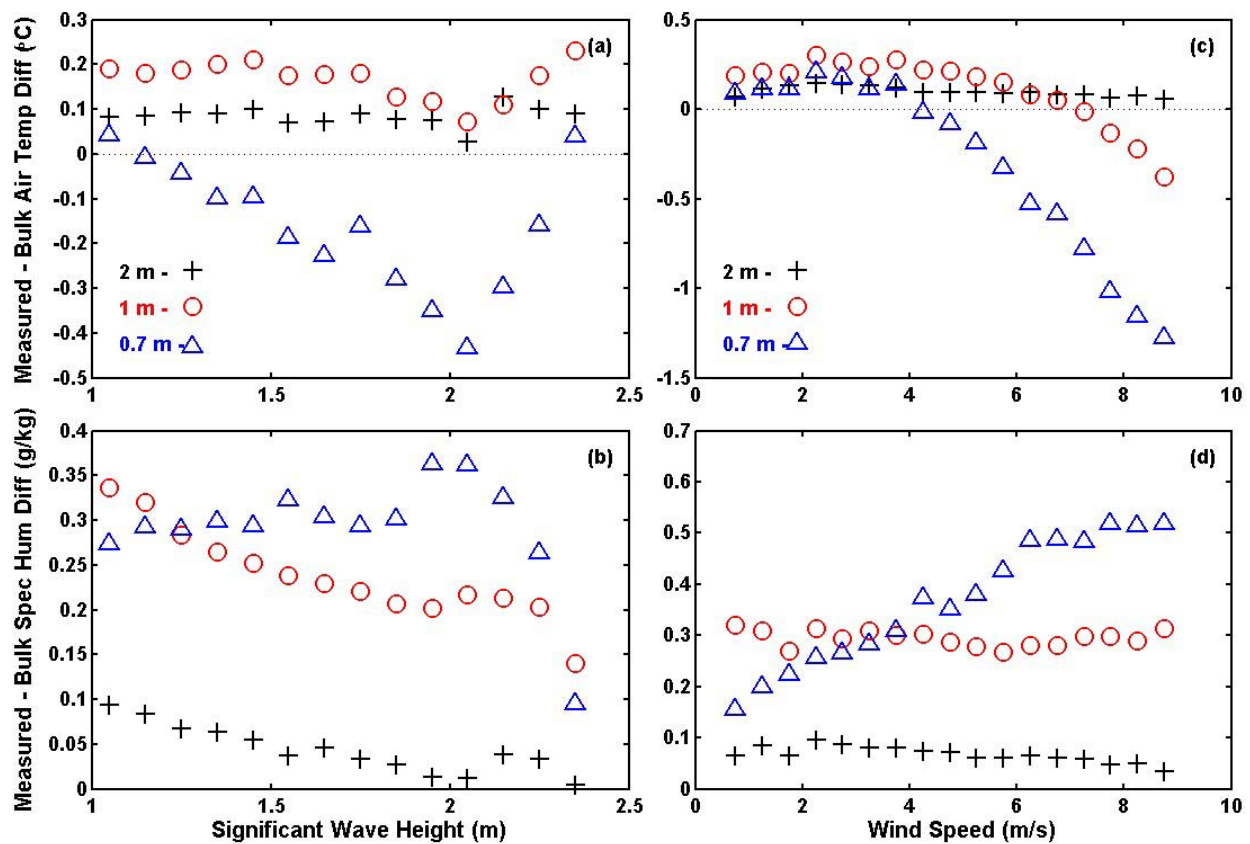


Figure 3. Plots showing bin-averaged values of measured – bulk model estimates of air temperature and specific humidity versus significant wave height and wind speed at the three buoy measurement height levels; 0.7 m (blue triangles), 1 m (red circles) and 2 m (black crosses).

2 m, 1 m and 0.7 m heights above the surface and corresponding bulk model estimates are plotted versus the significant wave height and the wind speed. The data shown in Figure 3 have been averaged within significant wave height and wind speed bins and only the average value within each bin is shown. The bulk profile estimates were computed using the buoy data from the 4 m level and the float thermistor sensors as inputs, therefore the bulk values at 4 m height are the same as the measured values and measured – bulk differences are computed only for the 2 m, 1 m and 0.7 m levels. In effect we are assuming that the 4 m height measurements are perfect and are above the wavy layer (i.e. above the region significantly influenced by surface waves).

Presumably the effect that ocean wave-induced turbulence and vertical mixing might have on scalar profiles would be greatest near the surface and decrease with height. These effects might also be expected to increase with either or both significant wave height (representing swell) and wind speed (representing wind-generated short waves). Therefore we would expect to see larger measured-bulk model differences close to the surface, which increase with H_s and/or wind speed. An examination of Figure 3

indicates some evidence of such a trend, especially in the plots of temperature and humidity differences versus wind speed at the 0.7 m level (blue triangles), and to a lesser extent the 1 m level. The deviation of the buoy measurements from the bulk model predictions at 2 m heights show little dependence upon either significant wave height or wind speed, indicating there is very little wave induced mixing at this height.

From Figure 3 we can see that for all three height levels and for the entire range of observed H_s and wind speed values, the measured specific humidity was greater than the bulk prediction. Assuming the sensors were properly calibrated, as we believe, this result could have different possible causes: due to enhanced wave-induced mixing near the surface which decreases the scalar gradients, or due to the temperature/humidity sensors becoming wet either from spray or by immersion from a large wave.

Spray droplet studies indicate that for the wind speeds encountered in this experiment (below 10 m/s) the impact of spray droplet evaporation on temperature and humidity is insignificant (Andreas et al. 1995). However, it is possible that the wind speed dependent measured-bulk differences observed at 0.7 m and also possibly at

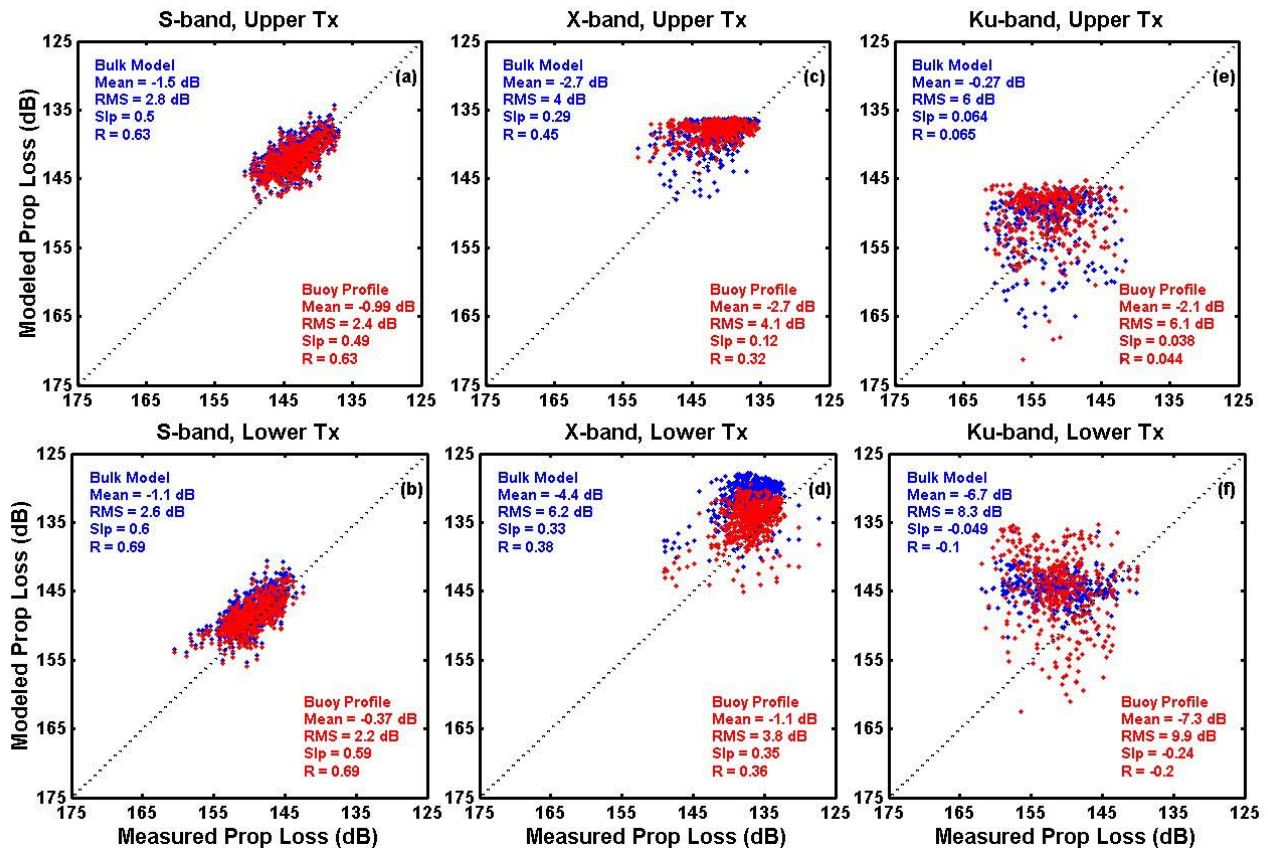


Figure 4. Scatter plots of APM modeled versus measured propagation loss using the NPS bulk model only (shown in blue) and the NPS buoy profile measurements up to 4 m and NPS model above (shown in red) as inputs to APM for both the upper (~13 m) and lower (~5 m) transmitters and all three frequencies.

the 1 m level are due to these low level sensors getting wet either from being completely dunked or from sea-spray. The sensors themselves were encased within radiation shields but even if water droplets accumulated on the radiation shield, the resulting evaporation could lead to cooler temperature and higher humidity values.

4.2 Propagation Results

Microwave frequency propagation depends upon the vertical profile of modified refractivity, which is primarily controlled by humidity, rather than temperature. The measured buoy profiles of modified refractivity showed exactly the same behavior as specific humidity, i.e. larger than estimated values and a reduced vertical gradient just above the surface. Indeed, the profile plots for modified refractivity are so similar to the specific humidity plots that they are not shown here.

APM propagation calculations were performed with two different modified refractivity profiles as inputs for every case: first with the NPS model profile alone, and second with the directly measured NPS buoy profile for heights below 4 m attached to the model profile above. Comparisons between the measured propagation loss and modeled values are displayed as scatter plots in Figure 4. The NPS model predictions alone are shown in blue and the buoy measured profile predictions are shown in red. The combined buoy and NPS profile APM predictions agreed better on average with the measurements for S-band and the lower X-band, while the NPS model alone agreed better for Ku-band. The higher frequencies (X-band and especially Ku-band) are much more sensitive than S-band to variations in the structure of the modified refractivity profile and also to surface wave scattering and reflection and are thus much more difficult to model accurately. The good agreement (less than 3 dB in RMS differences) between the measured and modeled propagation loss values in S-band is impressive. The higher frequency bands exhibit shadow zone behavior at the ranges and heights used in the RED Experiment and propagation loss can change rapidly with height and range, making it very difficult to model. The fact that in the mean the X- and Ku-band modeled values agree reasonably well with the measurements (and much better than standard atmosphere or free space predictions) is encouraging.

5. CONCLUSIONS

In this paper we have attempted to show the possible effects of ocean wave influences on near-surface scalar profiles and microwave propagation. The conditions encountered in this study were nearly ideal for the application of a bulk model based on MOS theory: conditions were steady and unstable (negative air-sea temperature difference) throughout, winds were moderate, the trade winds were constant from a westerly direction and the measurements were thus representative of the open ocean and free from land effects. The excellent agreement between the S-band measurements and modeled values is a good indicator

that the NPS bulk model performed well for the swell dominated and unstable conditions encountered during the RED Experiment. However, the fact that the modeled propagation loss computed from the directly measured buoy profiles produced the best agreement with the measurements for S- and X-bands indicates that the reduced humidity gradients observed from the buoy may be real and could be caused by enhanced wave-induced mixing near the surface.

ACKNOWLEDGEMENTS

The authors wish to thank Mr. Keith Jones for his efforts in buoy data collection. Dr. Ronald Ferek of the Office of Naval Research arranged funding for this work.

REFERENCES

- Anderson, K. D., P. A. Frederickson, E. Terrill, 2003: Air-Sea Interaction Effects on Microwave Propagation over the Sea during the Rough Evaporation Duct (RED) Experiment. *Proc., 12th Conf. on Interaction of the Sea and Atmosphere*, 9–13 February 2003, Long Beach, CA [Paper 9.1 of these proceedings].
- Andreas, E. L., J. B. Edson, E. C. Monahan, M. P. Rouault, and S. D. Smith, 1995: The spray contribution to net evaporation from the sea: A review of recent progress. *Bound.-Layer Meteorol.*, **72**, 3-52.
- Barrios, A., 2002: Advanced Propagation Model Version 1.31 CSCI Documents. SPAWARCYSCEN Tech. Doc. 3145, ?? pp.
- Fairall, C. W., E. F. Bradley, D. P. Rogers, J. B. Edson, and G. S. Young, 1996: Bulk Parameterization of Air-Sea Fluxes for Tropical Ocean-Global Atmosphere Coupled-Ocean Atmosphere Response Experiment. *J. Geophys. Res.*, **101** (C2), 3747-3764.
- Frederickson, P. A., K. L. Davidson, and A. K. Goroch, 2000: Operational evaporation duct model for MORIAH. *Naval Postgraduate School Report*, Draft version 1.2, May 2000, 70 pages.
- Hare, J. E., T. Hara, J. B. Edson, and J. M. Wilczak, 1997: A similarity analysis of the structure of airflow over surface waves. *J. Phys. Oceanogr.*, **27**, 1018-1037.
- Hirstov, T., C. Friehe, and S. Miller, 1998: Wave-coherent fields in air flow over ocean waves: Identification of cooperative behavior buried in turbulence. *Phys. Rev. Lett.*, **81**(2), 5245-5248.
- Liu, W. T., K. B. Katsaros, and J. A. Businger, 1979: Bulk parameterization of air-sea exchanges of heat and water vapor including the molecular constraints at the interface. *J. Atmos. Sci.*, **36**, 1722-1735.